Assessment of Differential Pulmonary Blood Flow Using Perfusion Magnetic Resonance Imaging

Comparison With Radionuclide Perfusion Scintigraphy

Francesco Molinari, MD, Christian Fink, MD,†‡ Frank Risse, PhD,§ Siegfried Tuengerthal, MD,¶ Lorenzo Bonomo, MD,* and Hans-Ulrich Kauczor, MD†*

Objectives: We sought to assess the agreement between lung perfusion ratios calculated from pulmonary perfusion magnetic resonance imaging (MRI) and those calculated from radionuclide (RN) perfusion scintigraphy.

Materials and Methods: A retrospective analysis of MR and RN perfusion scans was conducted in 23 patients (mean age, 60 ± 14 years) with different lung diseases (lung cancer = 15, chronic obstructive pulmonary disease = 4, cystic fibrosis = 2, and mesothelioma = 2). Pulmonary perfusion was assessed by a time-resolved contrast-enhanced 3D gradient-echo pulse sequence using parallel imaging and view sharing (TR = 1.9 milliseconds; TE = 0.8 milliseconds; parallel imaging acceleration factor = 2; partition thickness = 4 mm; matrix = 256 × 96; in-plane spatial resolution = 1.87 × 3.75 mm; scan time for each 3D dataset = 1.5 seconds), using gadolinium-based contrast agents (injection flow rate = 5 mL/s, dose = 0.1 mmol/kg of body weight). The peak concentration (PC) of the contrast agent bolus, the pulmonary blood flow (PBF), and blood volume (PBV) were computed from the signal-time curves of the lung. Left-to-right ratios of pulmonary perfusion were calculated from the MR parameters and RN counts. The agreement between these ratios was assessed for side prevalence (sign test) and quantitatively (Deming-regression).

Results: MR and RN ratios agreed on side prevalence in 21 patients (91%) with PC, in 20 (87%) with PBF, and in 17 (74%) with PBV. The MR estimations of left-to-right perfusion ratios correlated significantly with those of RN perfusion scans ($P < 0.01$). The correlation was higher using PC (r = 0.67) and PBF (r = 0.66) than using PBV (r = 0.50). The MR ratios computed from PBF showed the highest accuracy, followed by those from PC and PBV. Independently from the MR parameter used, in some patients the quantitative difference between the MR and RN ratios was not negligible.

Conclusions: Pulmonary perfusion MRI can be used to assess the differential blood flow of the lung. Further studies in a larger group of patients are required to fully confirm the clinical suitability of this imaging method.

Key Words: lung, magnetic resonance imaging (MRI), perfusion, blood flow, functional imaging

(*Invest Radiol* 2006;41: 624–630)

The feasibility of a noninvasive assessment of pulmonary perfusion by contrast-enhanced magnetic resonance imaging (MRI) has been demonstrated recently.[1–12] The advantages of this new imaging method over perfusion scintigraphy primarily include the higher spatial resolution and the additional temporal information about pulmonary blood flow. Moreover, pulmonary perfusion MRI may be performed in a 3D fashion with full coverage of both lungs.[4–8,10,12] Because of the potential capability to combine the perfusion measurements with morphologic MRI,[1] pulmonary perfusion MRI may be more accurate in characterizing the etiology of perfusion changes than perfusion scintigraphy. In addition, several studies have shown the feasibility of a quantitative analysis of pulmonary perfusion MRI by applying the indicator dilution theory.[2,3,10–13]

Some investigators[11,14] have recently proposed the use of pulmonary perfusion MRI to quantify the differential pulmonary blood flow in surgically treatable lung cancer patients, to estimate the postoperative residual lung function. In both studies, pulmonary perfusion MRI correlated well with radionuclide (RN) perfusion scans. However, some technical limitations included low temporal[14] and spatial[11] resolution.

In addition to lung cancer, the assessment of differential pulmonary blood flow is also of relevance in other clinical settings. In patients with Fontan-like circulation, such as in cavopulmonary shunts, preferential blood flow to one lung is caused by postsurgical anatomic changes and is of major prognostic relevance.[15,16] Another example is patients with single-lung transplantation, in whom the mean fraction of perfusion to the transplanted lung is considered a prognostic factor for chronic rejection.[17,18] Differential pulmonary per-

Received January 17, 2006, and accepted for publication, after revision, April 25, 2006.

From the *Department of Radiological Sciences, Catholic University of Rome, Rome, Italy; †Department of Radiology and §Medical Physics in Radiology, Deutsches Krebsforchungszentrum (DKFZ), Heidelberg, Germany; ‡Institute of Clinical Radiology Ludwig-Maximilians-University of Munich, University Clinics Grosshadern, Munich, Germany; and ¶Department of Radiology, Thoraxklinik, Heidelberg, Germany.

Drs. Molinari and Fink contributed equally to this work.

Reprints: Francesco Molinari, MD, Department of Radiological Sciences, Catholic University of Rome, Italy, L.go F. Vito n. 1, 00168 Rome, Italy. E-mail: fmolinari@rm.unicatt.it.

ISSN: 0020-9996/06/4108-0624

fusion has been also related to prognosis in lung volume reduction surgery for emphysema[19] and in the medical treatment of cystic fibrosis.[20,21] Finally, perfusion abnormalities with side prevalence have been reported in pulmonary vein stenosis after radiofrequency ablation for atrial fibrillation.[22–24]

In future, pulmonary perfusion MRI could be a valid alternative to perfusion scintigraphy for the assessment of differential pulmonary blood flow in all those clinical settings. The higher local resolution of MRI would enable a lobar or segmental based quantification of pulmonary perfusion, increasing the accuracy of the comparisons between pre and postoperative evaluations. In contrast to scintigraphy, additional information on the temporal distribution of pulmonary blood flow would be achieved from the same data, aiding the quantitative assessment of pulmonary shunts. The absence of ionizing radiation would also allow for performing short-term follow-up studies and for therapy monitoring. Therefore, the reliability of this imaging method in comparison to scintigraphy needs to be further investigated.

In this study, we evaluated the agreement between pulmonary perfusion MRI and perfusion scintigraphy in the assessment of differential pulmonary blood flow. Percentage ratios of pulmonary perfusion were calculated from semiquantitative MR data.

MATERIALS AND METHODS

Patients

The patients of this study were identified in the institutional database by a query performed over 2 years (from December 2003 to December 2005). The query resulted in an initial number of 176 patients with a perfusion MRI examination, which had been performed as a part of the imaging protocol of different clinical studies. The investigation protocols of these studies, including the perfusion MRI examination, were approved by the institutional human research ethic committee, and written informed consent was acquired from all patients. The informed consent included also the possibility of a retrospective analysis of the image data in a different context than the initial clinical study.

All 176 patients had been referred by one specialized hospital for chest diseases. Among them, we identified 23 patients who had been also examined by RN perfusion scintigraphy within 2 weeks from perfusion MRI (average = 6.5 days ± 5 SD). This maximum interval was accepted between the 2 imaging modalities to limit a bias resulting from variations of perfusion.

The pulmonary perfusion MRI and the RN perfusion scans of these 23 patients (17 men, 6 women, mean age 60 years ± 14 SD) were retrospectively analyzed. Patients' diagnosis was lung cancer (n = 15; 6 with upper sulcus tumor), chronic obstructive pulmonary disease (n = 4), cystic fibrosis (n = 2), and mesothelioma (n = 2).

MRI

All MRI examinations were performed on a 1.5 T whole-body scanner (Magnetom Symphony-Quantum, Siemens, Erlangen, Germany) offering a maximum gradient strength of 30 mT/m and a slew rate of 125 T/m/s. A combination of 2 spine array coils with 2 four-element body phased-array coils, or a 6-channel torso phased array coil, was used for signal reception. Patients were examined in a supine position.

Pulmonary perfusion was assessed by a time-resolved contrast-enhanced 3D gradient echo pulse sequence (fast low-angle shot; FLASH 3D) combining parallel imaging with view-sharing (TREAT).[25] Imaging parameters were: repetition time (TR) = 1.9 milliseconds; echo time (TE) = 0.8 milliseconds; flip angle = 40°; receiver bandwidth = 1220 Hz/pixel; GRAPPA; parallel imaging acceleration factor = 2; reference k-space lines for calibration = 20; echo-sharing factor = 3; spiral-radial reorder mode; field of view (FOV) = 480 × 360 mm; matrix = 256 × 96. The in-plane spatial resolution was 1.87 × 3.75 mm. Full coverage of the thorax was obtained in the coronal plane with a 176-mm thick 3D slab. A total of 44 partitions were reconstructed from this slab, resulting in a 4-mm partition thickness. The scan time for each 3D dataset was 1.5 seconds. Twenty consecutive datasets were acquired in 30 seconds of inspiratory breathhold. Patients were asked to hold their breath as long as possible during the data acquisition. Cardiac triggering or gating methods were not used.

Image acquisition was started with the beginning of contrast injection. Gadobenate dimeglumine (Multihance, Altana Pharma, Konstanz, Germany) or gadodiamide (Omniscan, Amersham Health-GE, Ismaning, Germany) was injected into a cubital vein using an automatic power injector at a rate of 5 mL/s with a body-weight-adapted dose of 0.1 mmol/kg body weight followed by a saline flush of 30 mL injected at the same injection rate.

Radionuclide Perfusion Imaging

Radionuclide lung perfusion scintigraphy was performed in all patients with a double-head unit (Axis; Philips Medical Systems, Best, Netherlands) and 80–120 MBq of technetium 99m–marked macroaggregated albumin (MAA Sol; Amersham Health-GE, Ismaning, Germany), which equaled an amount of about 200,000 particles. Image acquisition started immediately after injection of the tracer into a cubital vein. Planar perfusion images were acquired while patient was free-breathing in the supine position, in the following 8 projections: anterior, posterior, left anterior oblique, right anterior oblique, left posterior oblique, right posterior oblique, and both lateral projections. In each projection, 400,000 counts were registered. Each RN perfusion scan lasted 15 to 20 minutes.

MR Data Analysis

Pulmonary perfusion MRI was analyzed using an in-house-developed software based on Interactive Data Language (IDL; Research Systems, Boulder, CO), which was implemented on a conventional PC platform (Intel Pentium IV 2.6 GHz computer, with 1 GB RAM).

The arterial input function was determined placing a region of interest (ROI) in the main pulmonary artery. Next, both lungs were outlined by manually drawn ROIs in all partitions of the 3D dataset. The outmost partitions were excluded for the presence of infolding artifacts. An average

number of 24 partitions was used for the data analysis (range, 17–31 slices). Signal-time curves were calculated for each ROI, using the average of the signal intensity values of the pixels included in the ROI. The baseline, the bolus and the recirculation phase in the plot were automatically delimited by the software. When the algorithm failed to recognize those phases, manual delimitation was used. The overall processing phase took about 30 to 45 minutes per examination. As previously described,[2,3,9–13] perfusion was quantified from pulmonary perfusion MRI using the indicator dilution theory. Briefly, assuming a linear relation between the signal and the concentration of contrast agent (although this was not an intravascular one), signal-time curves were converted to concentration-time curves. From these curves, the peak concentration (PC [a.u.]) of the contrast agent bolus was obtained. After applying the indicator dilution theory, the regional pulmonary blood flow (PBF [mL/100 mL lung tissue/min]) and pulmonary blood volume (PBV [mL/100 mL lung tissue]) were computed as parametric data.[26]

These parameters were computed and color-coded for each pixel in the ROI. For each ROI, all parameters represented means of the corresponding pixel values. The contribution of the high signal of contrast medium in the distal pulmonary vessels to mean parametric values was excluded using cross correlation analysis.[27]

Left-to-right MR perfusion ratios were calculated using PC, PBF, and PBV values. Mean values of these parameters obtained from each partition were averaged among all partitions matching the same side. MR perfusion ratios were compared with left-to-right RN perfusion ratios.

RN Data Analysis

The relative percentage of left and right counts over global counts was calculated from the anterior and posterior projections using the software provided with the scintigraphy unit. RN ratios were computed as a standard reference.

Statistical Analysis

To assess the agreement in defining the left or right prevalence of perfusion, in each patient all calculated MR perfusion ratios were first compared with the corresponding RN ones using the sign test (L/R $>$ 1 [left prevalence of perfusion]; L/R $<$ 1 [right prevalence of perfusion]; L/R = 0 [side equivalence of perfusion]; y = agreement between MR and RN ratios; n = no agreement).

Each MR ratio was then plotted against the corresponding RN one. To estimate the quantitative differences between MR ratios (test method) and RN ratios (comparative method), both methods were considered as affected by random error. Therefore, the Deming regression (Dr)[28] was used to calculate the linear regression equation with its coefficient of correlation (r), the parameters of the model (b_{Dr} = slope; a_{Dr} = intercept) and their 95% confidence intervals. Student t-statistic was used to test the statistical significance of r and of the differences between the parameters of the Dr line (b_{Dr} and a_{Dr}) and the line of identity (id line, b_{id} [slope of the line of identity] = 1; a_{id} [intercept of the line of identity] = 0). A *P* value of less than 0.05 was considered as significant in all statistical data. Statistical analysis was performed with Excel 2003 (Microsoft Corp., Redmond, WA) and MedCalc (MedCalc Software, Mariakerke, Belgium).

RESULTS

The agreement between the side prevalence of MR and RN ratios (ie, left or right) is shown in Table 1. The side prevalence of RN ratios was correctly estimated in 21 patients by PC (91%; $P < 0.01$), in 20 by PBF (87%; $P < 0.01$), and in 17 by PBV (74%; $P < 0.01$). In 2 patients (No. 10 and 15, Table 1), the RN ratios were greater than 0.95 indicating only a small prevalence of right over left perfusion, whereas the corresponding MR ratios differed slightly from the RN ones (PC = 1.05; PBF = 1.05; PBV = 1.00 for patient No. 10; PBF = 1.05 for patient No. 15, Table 1). Considering these slight differences, the side prevalence was incorrectly estimated by PC and PBF only in one patient (No. 23, mesothelioma, Table 1).

Examples of MR and RN perfusion maps of 2 patients are shown in Figures 1 and 2. In Figure 1, in a patient with lung cancer, a good agreement is shown between the left-to-

TABLE 1. Perfusion Ratios Calculated From Magnetic Resonance (MR) Parameters and Radionuclide (RN) Counts

No.	PC		PBF		PBV		RN Counts	
1	0.77	R	0.74	R	0.79	R	0.85	R
2	0.56	R	0.53	R	0.63	R	0.63	R
3	0.79	R	0.92	R	0.77	R	0.79	R
4	0.57	R	0.58	R	0.58	R	0.90	R
5	0.20	R	0.13	R	0.42	R	0.23	R
6	0.79	R	0.85	R	0.84	R	0.61	R
7	0.82	R	0.80	R	1.09[2]	L*	0.54	R
8	0.86	R	0.86	R	0.94	R	0.87	R
9	0.69	R	0.64	R	0.69	R	0.66	R
10	1.05[1]	L*	1.05[1]	L*	1.00[1]	L = R*	0.97	R
11	0.82	R	0.86	R	0.82	R	0.91	R
12	0.42	R	0.24	R	0.35	R	0.23	R
13	0.85	R	0.78	R	0.86	R	0.92	R
14	1.14	L	1.64	L	0.92[2]	R*	1.13	L
15	0.94	R	1.05[1]	L*	0.94	R	0.98	R
16	1.07	L	1.17	L	0.90[2]	R*	1.24	L
17	0.84	R	0.81	R	0.82	R	0.49	R
18	0.97	R	0.95	R	1.01[2]	L*	0.70	R
19	0.73	R	0.74	R	0.71	R	0.78	R
20	0.88	R	0.92	R	0.93	R	0.40	R
21	0.71	R	0.72	R	0.81	R	0.70	R
22	1.17	L	1.24	L	1.10	L	1.16	L
23	0.85[2]	R*	0.84[2]	R*	0.85[2]	R*	1.50	L

The numbers in the PC, PBF, and PBV column represent the left-to-right ratios of pulmonary perfusion computed from the MR parameters indicated in the column header. The corresponding left-to-right ratios calculated from RN counts are shown in the last column. All letters marked with an asterisk (*) represent MR ratios that disagreed for side prevalence from the corresponding RN ones. For instance, in patient no. 7 the MR ratio computed from PBV showed higher perfusion on the left (ratio $>$ 1, L), whereas the corresponding RN ratios showed higher perfusion on the right (ratio $<$ 1, R). Among the MR ratios in disagreement with the RN ones, those marked with [1] showed a quantitative differences from the RN ratios comprised within 0.10, whereas those marked with [2] showed a larger quantitative differences ($>$ 0.10).

PC, peak concentration; PBF, pulmonary blood flow; PBV, pulmonary blood volume; R, right prevalence of pulmonary perfusion; L, left prevalence of pulmonary perfusion.

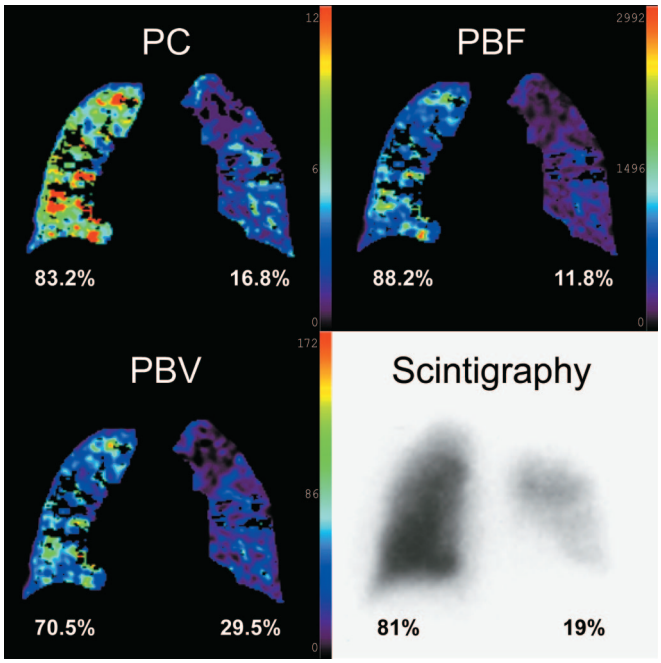

FIGURE 1. Magnetic resonance and radionuclide perfusion maps in a patient with lung cancer of the right hilum (patient no. 5). Good agreement was found for side prevalence, distribution, and quantitative values between MR and RN perfusion ratios. Each pixel in the MR maps is color-coded according to the computed parametric value. PC = peak concentration (a.u.); PBF = pulmonary blood flow (mL/100 mL lung tissue/min); PBV = pulmonary blood volume (mL/100 mL lung tissue). The percentages reported under the RN perfusion image represent the distribution of the total counts in both lungs (ie, 81% of total counts on the right and 19% on the left). Similarly, the percentages reported under the MR perfusion maps refer to the distribution of the global values of the corresponding MR perfusion parameters in both lungs (see Materials and Methods). The MR maps represent the partitions whose results on the side distribution of the relative perfusion parameters best approximated the reported global ones. The defects in the MR maps are either due to vessels automatically removed by the software or to very low parametric values. Clearly pulmonary perfusion is higher on the right side, predominantly in the lower lobe. Left upper lobe is hypoperfused in all MR and RN maps due to hilar tumor.

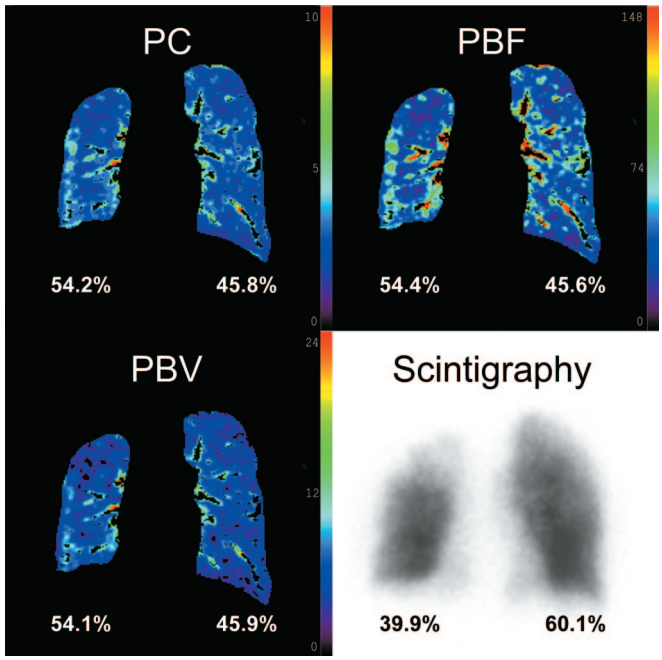

FIGURE 2. Magnetic resonance and radionuclide perfusion maps in a patient with right mesothelioma (patient no. 23). MR and RN perfusion ratios disagreed for both side prevalence and quantitative values. Lung volume on the right side is reduced for restricted expansion of the hemithorax. PC = peak concentration (a.u.); PBF = pulmonary blood flow (mL/100 mL lung tissue/min); PBV = pulmonary blood volume (mL/100 mL lung tissue). See also Figure 1 for the meaning of the percentages and the MR perfusion maps.

right perfusion ratio computed from scintigraphy (ratio = 0.23, with 19% of global perfusion on the left and 81% on the right) and those from pulmonary perfusion MRI (ratio = 0.20 for PC, 0.13 for PBF and 0.42 for PBV). The defects in all MR parametric maps express either vessels removed by the software or very low parametric values. Pulmonary perfusion is higher on the right side, predominantly in the lower lobe. The left upper lobe is hypoperfused in the MR and RN perfusion maps due to left hilar tumor. Conversely, no agreement was found in a patient with mesothelioma (Fig. 2). In fact, all MR perfusion maps show the prevalence of perfusion on the right side (left-to-right ratio = 0.85 for PC, 0.84 for PBF and 0.85 for PBV) whereas on scintigraphy perfusion prevails on the left (left-to-right ratio = 1.50, with 60% of global perfusion on the left and 40% on the right). Right lung volume is reduced probably by pleural tumor thickening.

The Dr scatter-plots and the parameters of the Dr analysis are shown in Figure 3. A significant-but-moderate correlation was found between all MR and RN ratios, with slight differences among the r values (r = 0.67 for PC; r = 0.66 for PBF; r = 0.50 for PBV). The slopes and the intercepts of the Dr lines were not significantly different from the slope and the intercept of the line of identity. The MR ratios computed from PBF showed the highest accuracy (b_{Dr} = 0.99 versus b_{id} = 1, a_{Dr} = −0.03 vs. a_{id} = 0). Independently from the MR parameter used, in some patients the quantitative difference between the MR and RN ratios was not negligible (Table 1 and Fig. 3). Therefore, the 95% confidence intervals for the slopes and the intercepts resulted wide for all 3 MR parameters.

DISCUSSION

The assessment of differential pulmonary blood flow is of clinical interest in a variety of lung diseases.[15–24,29] Perfusion scintigraphy is commonly used to quantify the distribution of pulmonary blood flow. In this study, we have proposed pulmonary perfusion MRI as an alternative imaging method to estimate differential pulmonary blood flow in lung disease. In detail, left-to-right ratios of pulmonary perfusion

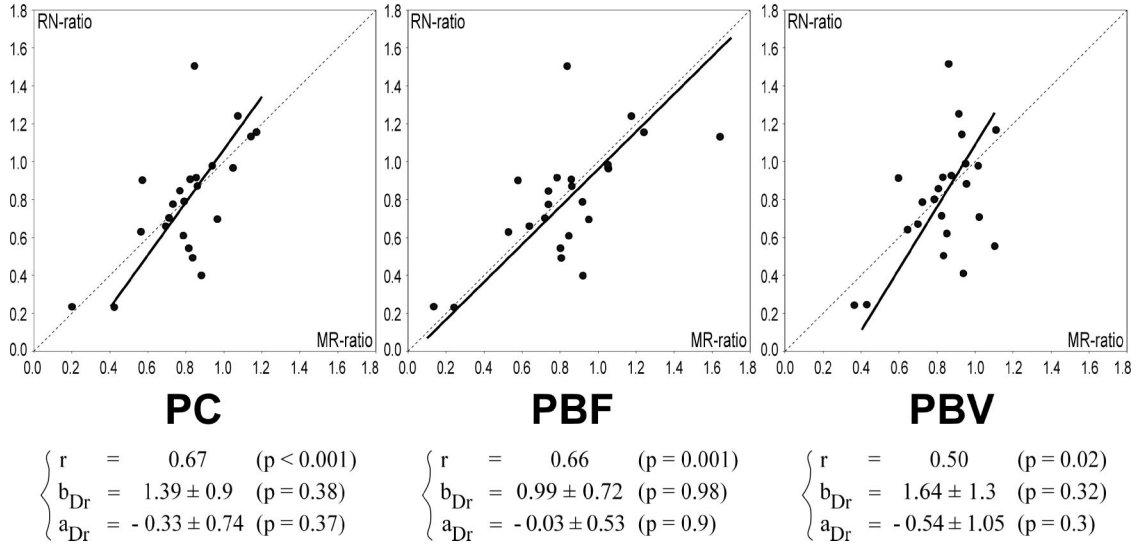

FIGURE 3. Deming regression applied to the comparison of magnetic resonance (MR) and radionuclide (RN) perfusion ratios. MR ratios were calculated from peak concentration (PC [a.u.]), pulmonary blood flow (PBF [mL/100 mL lung tissue/min]), and pulmonary blood volume (PBV [mL/100 mL lung tissue]). In each graph, the dotted line represents the line of identity and the solid line represents the Deming regression (Dr). r = correlation coefficient; b_{Dr} = slope of the Dr line with its confidence interval; and a_{Dr} = intercept of the Dr line with its confidence interval. If the ratios of pulmonary perfusion computed from those 3 MR parameters were perfectly matching with those computed from the RN counts in all patients, all dots should lie on the line of identities and the Dr lines should have intercept and slope identical to the line of identity. The p values for the correlation coefficients indicate their statistical significance. The p values for the slopes and the intercepts of the Dr lines represent the results of the Student t-statistic applied to their respective differences from the slopes and the intercepts of the identity lines. With all 3 parameters, b_{Dr} and a_{Dr} are not significantly different from the slope and the intercept of the identity line. However, the Dr line computed from PBF almost matches with the line of identity indicating higher accuracy of the MR ratios of pulmonary perfusion calculated from PBF than those from PC and PBF.

were calculated from semiquantitative MR perfusion parameters and were compared with perfusion scintigraphy.

In our study, the side prevalence of lung perfusion was estimated correctly by pulmonary perfusion MRI in most of the patients; PC and PBF were found to be more accurate than PBV. Similarly, all 3 MR estimations of left-to-right perfusion ratios correlated quantitatively with those of RN perfusion scans. The correlation was slightly higher using PC and PBF than using PBV. The MR perfusion ratios computed from PBF showed high accuracy. However, in consideration of all 3 MR parameters, the quantitative difference between the MR and RN ratios was not negligible in some patients.

In most patients with lung cancer, MR and RN perfusion ratios had a good or excellent agreement. In contrast, the widest differences among these ratios were found in both patients with mesothelioma, in 3 of 6 patients with superior sulcus tumor, and in 1 patient with cystic fibrosis. In all these patients, a large difference between the volumes of the left and right lung was observed at end-inspiratory breath-hold. In those patients with mesothelioma and superior sulcus tumor, lesser lung volume was invariably linked to tumor location, suggesting mechanical limitation to chest wall expansion. In the patient with cystic fibrosis the restricted expansion of one lung may be explained by asymmetric fibrotic changes. In contrary to perfusion scintigraphy, in all these patients MRI showed a consistently higher perfusion in the less expanded lung. Recently, 2 studies have demonstrated that pulmonary perfusion obtained by MRI is modulated by volume differences, such as those occurring in inspiratory and expiratory breath-hold.[13,30] In both studies, perfusion was higher in less inflated lung, consistent with the opening of the microvessels, which occurs in expiration, when lung-tissue stretching lowers. In addition, the baseline signal intensity of the lung is also modulated by lung volume.[31] In fact, lung deflation reduces the number of alveolar air-tissue interfaces leading to lower magnetic-field inhomogeneity and less signal dispersion due to magnetic susceptibility T2*-effects.[32,33]

In conditions in which large volume differences between the left and right lung occur, both phenomena might be involved in determining a higher fraction of perfusion to the less expanded lung. Those volume differences might have become even larger in our study, because pulmonary perfusion MRI was performed during inspiratory breath-hold. Moreover, this level of inflation was obtained with a single deep inspiration, immediately followed by the MR contrast injection. Therefore, at the arrival of the contrast in the pulmonary microvessels, the distribution of peripheral blood flow might have been influenced by capillary pressure differences secondary to those of lung volumes. Conversely, perfusion scintigraphy was performed by injection of the macroaggregates followed by multiple deep inspirations. Hence, in perfusion scintigraphy the inflow mechanism would lead to a random distribution of the macroaggregates which would reach the capillary bed before pressure related constriction of

the capillaries. Finally, because of the longer acquisition time, perfusion scintigraphy was performed during shallow breathing at an average level of inflation. For those reasons, perfusion scintigraphy might not reflect the side predominance detected by perfusion MRI in the above mentioned patients.

Higher correlation coefficients between MR and RN perfusion ratios have been reported recently in 2 articles.[11,14] Some differences from both studies could explain our partly contradictive results. First, the method used to calculate MR ratios was different from our study. Iwasawa et al[14] computed these ratios using the peak signal intensity measured from the left and right lung after contrast administration. Initially, they multiplied the mean value of the peak signal intensity obtained from each ROI by its area. Next, they summed all these partial results to obtain the global value of peak signal intensity for each lung. Ohno et al[11] computed the MR ratios using an estimation of the pulmonary blood flow obtained from the quantitative analysis of the signal-time curves of the lung. Those curves were generated initially for each ROI drawn in each partition. The corresponding values of pulmonary blood flow were then summed to obtain the global value of perfusion. Both methods theoretically approximate the sum of counts performed in perfusion scintigraphy. In our study, the signal-time curves were calculated from the average of the signal intensity values of the pixels included in the ROIs. The MR quantitative parameters computed from those curves, therefore, represented mean values. By summing up parametric data that are expressed as means, we would have used a mathematical approach, whose physiological significance has not been demonstrated yet. Moreover, by applying the method used by Iwasawa et al,[14] which also considered the areas of the ROIs, for some patients of our study, we obtained results of global PBF and PBV not consistent with any possible perfusion parameter. Therefore, for the final calculation of the 3 MR parameters of perfusion in our study, we preferred to further average the mean parametric data obtained from each ROI, separately for the left and right lung. Of course, it must be considered that using this method different quantities are compared (means of MR data versus sums of RN counts).

Second, the MR imaging technique used in our study was not fully comparable with those of the previous studies. In the study from Iwasawa et al,[14] the voxel size was in the range of 75.7–156.6 mm^3 and only 3 consecutive volumetric datasets with a temporal resolution of 6–7 seconds per dataset could be acquired. In the study from Ohno et al,[11] the nominal voxel size was still in the range of 115.4–160 mm^3, but the temporal resolution was higher (1 second per dataset). Using a combination of parallel imaging with view-sharing,[25] we were able to obtain a substantially smaller voxel size (28.1 mm^3) with a temporal resolution of only 1.5 seconds per volumetric dataset. Finally, those studies were performed for a different purpose, the estimation of postoperative lung function. Therefore, their results are limited to the group of lung cancer patients.

Study Limitations

The calculation of the perfusion parameters is based on several assumptions. The theoretical limits of applying the quantitative model of tissue perfusion to dynamic contrast-enhanced MRI of the lung have been already described.[2,3,10–13,34–36] These limitations essentially concern the assumption of a linear relationship between the MR signal intensity and local contrast agent concentrations, which may be present only for a limited dose range.[3,12] In our study, the dose was primarily optimized for the image quality, which may be poor, especially in patients with chronic obstructive pulmonary disease. Thus, the results might be affected by saturation effects. In addition, the used calculation of perfusion parameters assumes the use of an intravascular tracer, which is not fulfilled for all conventional extracellular MR contrast agents. Especially in lung pathology such as lung tumors or mesothelioma, where the contrast agent may show extensive extravasation during the first pass, this could be a potential source of bias. To limit this bias, we excluded central or pleural based tumors from the calculation of signal-time curves. However, less-peripheral intrapulmonary lung tumors could not be excluded from this analysis. In these patients, the MR perfusion parameters were therefore potentially hampered by the influence of tumor perfusion. This potential bias has not been considered by any of the previous studies and needs further investigation.

A technical limitation in this study was that the outmost partitions of the 3D datasets, hampered by infolding artifacts, were discharged. Although those partitions most frequently covered small portions of the anterior and posterior aspects of the lung, this limited amount of parenchyma could not be included in the quantitative assessment of the MR perfusion parameters.

Finally, the assessment of differential pulmonary blood flow might also be performed using phase-contrast (PC) MRI.[37–39] However, the flow measurements performed in the main pulmonary arteries using PC-MRI do not necessary correlate with the parameters of perfusion assessed regionally (ie, pulmonary perfusion MRI or scintigraphy).[13,15] Therefore, other sources of error would have been introduced by using PC-MRI as comparative method.

CONCLUSION

Our results indicate that differential perfusion of the lung can be assessed by pulmonary perfusion MRI. However, some potential sources of errors in this approach need to be investigated to fully confirm its clinical suitability. By addressing these issues, the quantification of differential pulmonary blood flow may further improve and pulmonary perfusion MRI might be more accurate.

ACKNOWLEDGMENTS

The authors thank Tristan Anselm Kuder for technical assistance in the software program development.

REFERENCES

1. Hatabu H, Gaa J, Kim D, et al. Pulmonary perfusion: qualitative assessment with dynamic contrast-enhanced MRI using ultra-short TE and inversion recovery turbo FLASH. *Magn Reson Med*. 1996;36:503–508.
2. Hatabu H, Tadamura E, Levin DL, et al. Quantitative assessment of pulmonary perfusion with dynamic contrast-enhanced MRI. *Magn Reson Med*. 1999;42:1033–1038.

3. Levin DL, Chen Q, Zhang M, et al. Evaluation of regional pulmonary perfusion using ultrafast magnetic resonance imaging. *Magn Reson Med*. 2001;46:166–171.
4. Matsuoka S, Uchiyama K, Shima H, et al. Detectability of pulmonary perfusion defect and influence of breath holding on contrast-enhanced thick-slice 2D and on 3D MR pulmonary perfusion images. *J Magn Reson Imaging*. 2001;14:580–585.
5. Zheng J, Carr J, Harris K, et al. Three-dimensional MR pulmonary perfusion imaging and angiography with an injection of a new blood pool contrast agent B-22956/1. *J Magn Reson Imaging*. 2001;14:425–432.
6. Carr JC, Laub G, Zheng J, et al. Time-resolved three-dimensional pulmonary MR angiography and perfusion imaging with ultrashort repetition time. *Acad Radiol*. 2002;9:1407–1418.
7. Fink C, Bock M, Puderbach M, et al. Partially parallel three-dimensional magnetic resonance imaging for the assessment of lung perfusion–initial results. *Invest Radiol*. 2003;38:482–488.
8. Fink C, Puderbach M, Bock M, et al. Regional lung perfusion: assessment with partially parallel three-dimensional MR imaging. *Radiology*. 2004;231:175–184.
9. Fink C, Risse F, Buhmann R, et al. Quantitative analysis of pulmonary perfusion using time-resolved parallel 3D MRI—initial results. *Rofo*. 2004;176:170–174.
10. Ohno Y, Hatabu H, Murase K, et al. Quantitative assessment of regional pulmonary perfusion in the entire lung using three-dimensional ultrafast dynamic contrast-enhanced magnetic resonance imaging: preliminary experience in 40 subjects. *J Magn Reson Imaging*. 2004;20:353–365.
11. Ohno Y, Hatabu H, Higashino T, et al. Dynamic perfusion MRI versus perfusion scintigraphy: prediction of postoperative lung function in patients with lung cancer. *AJR Am J Roentgenol*. 2004;182:73–78.
12. Nikolaou K, Schoenberg SO, Brix G, et al. Quantification of pulmonary blood flow and volume in healthy volunteers by dynamic contrast-enhanced magnetic resonance imaging using a parallel imaging technique. *Invest Radiol*. 2004;39:537–545.
13. Fink C, Ley S, Risse F, et al. Effect of inspiratory and expiratory breathhold on pulmonary perfusion: assessment by pulmonary perfusion magnetic resonance imaging. *Invest Radiol*. 2005;40:72–79.
14. Iwasawa T, Saito K, Ogawa N, et al. Prediction of postoperative pulmonary function using perfusion magnetic resonance imaging of the lung. *J Magn Reson Imaging*. 2002;15:685–692.
15. Fratz S, Hess J, Schwaiger M, et al. More accurate quantification of pulmonary blood flow by magnetic resonance imaging than by lung perfusion scintigraphy in patients with fontan circulation. *Circulation*. 2002;106:1510–1513.
16. Roman KS, Kellenberger CJ, Farooq S, et al. Comparative imaging of differential pulmonary blood flow in patients with congenital heart disease: magnetic resonance imaging versus lung perfusion scintigraphy. *Pediatr Radiol*. 2005;35:295–301.
17. Hardoff R, Steinmetz AP, Krausz Y, et al. The prognostic value of perfusion lung scintigraphy in patients who underwent single-lung transplantation for emphysema and pulmonary fibrosis. *J Nucl Med*. 2000;41:1771–1776.
18. Bjortuft O, Simonsen S, Geiran OR, et al. Pulmonary haemodynamics after single-lung transplantation for end-stage pulmonary parenchymal disease. *Eur Respir J*. 1996;9:2007–2011.
19. Wang SC, Fischer KC, Slone RM, et al. Perfusion scintigraphy in the evaluation for lung volume reduction surgery: correlation with clinical outcome. *Radiology*. 1997;205:243–248.
20. Stanchina ML, Tantisira KG, Aquino SL, et al. Association of lung perfusion disparity and mortality in patients with cystic fibrosis awaiting lung transplantation. *J Heart Lung Transplant*. 2002;21:217–225.
21. Itti E, Fauroux B, Pigeot J, et al. Quantitative lung perfusion scan as a predictor of aerosol distribution heterogeneity and disease severity in children with cystic fibrosis. *Nucl Med Commun*. 2004;25:563–569.
22. Robbins IM, Colvin EV, Doyle TP, et al. Pulmonary vein stenosis after catheter ablation of atrial fibrillation. *Circulation*. 1998;98:1769–1775.
23. Kluge A, Dill T, Ekinci O, et al. Decreased pulmonary perfusion in pulmonary vein stenosis after radiofrequency ablation: assessment with dynamic magnetic resonance perfusion imaging. *Chest*. 2004;126:428–437.
24. Yang M, Akbari H, Reddy GP, et al. Identification of pulmonary vein stenosis after radiofrequency ablation for atrial fibrillation using MRI. *J Comput Assist Tomogr*. 2001;25:34–35.
25. Fink C, Ley S, Kroeker R, et al. Time-resolved contrast-enhanced three-dimensional magnetic resonance angiography of the chest: combination of parallel imaging with view sharing (TREAT). *Invest Radiol*. 2005;40:40–48.
26. Meier P, Zierler KL. On the theory of the indicator-dilution method for measurement of blood flow and volume. *J Appl Physiol*. 1954;6:731–744.
27. Risse F, Fink C, Kuder TA, et al. Suppression of pulmonary vasculature in quantitative lung perfusion MRI. *MAGMA*. 2004;17:208.
28. Cornbleet PJ, Gochman N. Incorrect least-squares regression coefficients in method-comparison analysis. *Clin Chem*. 1979;25:432–438.
29. O'Sullivan J, Hasan A, Mitchell L, et al. Differential pulmonary flow after heart transplantation in patients with malposition of the great arteries. *J Heart Lung Transplant*. 1997;16:1168–1170.
30. Mai VM, Chen Q, Bankier AA, et al. Effect of lung inflation on arterial spin labeling signal in MR perfusion imaging of human lung. *J Magn Reson Imaging*. 2001;13:954–959.
31. Bankier AA, O'Donnell CR, Mai VM, et al. Impact of lung volume on MR signal intensity changes of the lung parenchyma. *J Magn Reson Imaging*. 2004;20:961–966.
32. Bergin CJ, Glover GH, Pauly JM. Lung parenchyma: magnetic susceptibility in MR imaging. *Radiology*. 1991;180:845–848.
33. Cutillo AG, Ganesan K, Ailion DC, et al. Alveolar air-tissue interface and nuclear magnetic resonance behavior of lung. *J Appl Physiol*. 1991;70:2145–2154.
34. Weisskoff RM, Chesler D, Boxerman JL, et al. Pitfalls in MR measurement of tissue blood flow with intravascular tracers: which mean transit time? *Magn Reson Med*. 1993;29:553–558.
35. Donahue KM, Weisskoff RM, Burstein D. Water diffusion and exchange as they influence contrast enhancement. *J Magn Reson Imaging*. 1997;7:102–110.
36. Jerosch-Herold M, Wilke N, Stillman AE. Magnetic resonance quantification of the myocardial perfusion reserve with a Fermi function model for constrained deconvolution. *Med Phys*. 1998;25:73–84.
37. Pelc NJ, Herfkens RJ, Shimakawa A, et al. Phase contrast cine magnetic resonance imaging. *Magn Reson Q*. 1991;7:229–254.
38. Silverman JM, Julien PJ, Herfkens RJ, et al. Quantitative differential pulmonary perfusion: MR imaging versus radionuclide lung scanning. *Radiology*. 1993;189:699–701.
39. Lee VS, Spritzer CE, Carroll BA, et al. Flow quantification using fast cine phase-contrast MR imaging, conventional cine phase-contrast MR imaging, and Doppler sonography: in vitro and in vivo validation. *AJR Am J Roentgenol*. 1997;169:1125–1131.